Journal of Hydraulic Structures
J. Hydraul. Struct., 2022; 8(3):17-32
DOI: 10.22055/jhs.2022.41058.1216

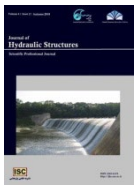

OPEN ACCESS

Numerical Study of Flow Characteristics Over Pivot Weirs

Bijan Khatamipour [1]
Mohammad Reza Kavianpour [2]
Amir Khosrojerdi[1]
Majid GhodsiHassanabad[3]

Abstract

Pivot weirs have a lifting mechanism to change the weir angle relative to the channel bed. These are installed across the waterways in the form of multiple weirs in a row. The water level will be adjusted by changing the weir angle. In this study, the flow over the pivot weirs was simulated with different flow discharges and angles using Ansys CFX model to investigate the flow characteristics. The model was evaluated using USBR experimental data. The standard K-ε turbulence model was considered as the best model for numerical analysis. According to the results, discharge coefficient increases with the inclination angle up to 1.076. The results showed a slight difference in comparison with the previous studies where values of 1.121, 1.110 and 1.082 were presented. The discharge coeffdwicient equations were developed for the weirs. The equations for various hydraulic parameters, including upstream water depth, water head on the crest, the ratio of water head over the crest to the weir height, and weir angle were developed. Based on the developed equations, the operation of the weirs was analyzed during flood events.

Keywords: Numerical model, Pivot weir, Ansys CFX, K-ɛ model, Inclined weir.

Received: 9 June 2022; Accepted: 5 September 2022

1. Introduction

The pivot weirs are the most important hydraulic structures that are used in many water resources projects to control the flow, especially during drought or flood events (when the water level changes sharply). In addition, the weirs are able to discharge the upstream accumulated sediments to the downstream. Pivot weirs are a type of movable weirs, which are the combination

[1] Department of Agricultural Systems Engineering, Faculty of Agricultural Sciences and Food Industry, Science and research Branch, Islamic Azad University, Tehran, Iran.
[2] Department of Water Engineering, Faculty of Civil Engineering, K.N. Toosi University of Technology, Iran. Email: kavianpour@kntu.ac.ir **(Corresponding Author)**
[3] Department of Marine Industries, Faculty of Engineering, Islamic Azad University, Science and Research Branch, Tehran, Iran.

of a plate, hydraulic jacks, support base and hydraulic cylinders (Figure 1). They have the ability to connect the remote control systems, to quickly open and close.

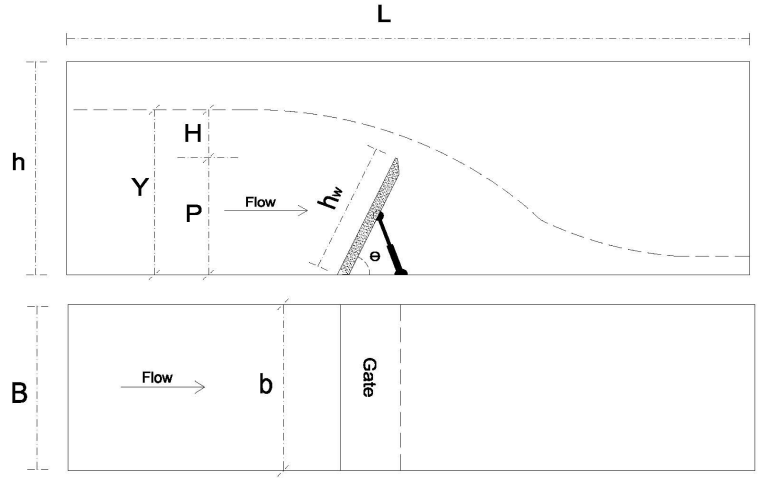

Figure 1. Plan and Profile of canal and pivot weir

The general flow discharge equation for vertical sharp-crested weirs is as follows:

$$Q=[\![2/3.C_d.\sqrt{2}g.b.H]\!]^{(3/2)} \quad (1)$$

where, C_d is the discharge coefficient, b is the weir length (m), H is the water head over the weir (m) and Q is the flow discharge (m^3/s). The discharge coefficient it was initially estimated to be 0.65 [1]. Extensive studies on the C value had been carried out by Rehbock [2], Bos [3] and Sisman [4] on sharp-crested weir with different side contraction. Sisman [4] observed that for water height below 2 cm, water clings to the lower nappe with non-aerated flow condition. Thus, water head on the weir below 2 cm was not taken into consideration. Hulsing [5] studied rectangular sharp-crested weirs without side contraction and presented the discharge-head curves with upstream weir slope ratio of 3:3, 2:3, 1:3, and 0:3 (Horizontal: Vertical). He found that, for a constant water head ratio (equal H/P ratio), the discharge coefficient increases with decreasing the slope of the weir. Swamee [6] provided a criterion for controlling the type of weir based on the ratio of the water head (H) to the crest thickness (t). According to his research, for H/t>1.5, the weir will act as a sharp-crested weir. Kindsvater and Carter [7] eliminated the effect of viscosity and surface tension for vertical sharp-crested weirs and used the C_e as discharge coefficient. The viscous and surface tension forces were accounted for by modifying the width of the weir and the head approaching the weir. They stated that if the correction factor for the angle (C_a) is estimated and then multiplied by vertical sharp-crested weirs formula, the obtained equation can be used for angular sharp-crested weirs. In this regard, Wahlin and Replogle [8] performed experimental studies (with USBR support) on two types of pivot weirs and developed equations for free flow conditions. Experiments have been performed on Armtec gates with 7 angles (varying from 16.2 to 63.4 degrees), and different side contractions for submerged and free flow conditions. They proposed, the flow discharge equation as follow:

$$Q = 2/3, C_a, C_r, C_d, \sqrt{2g}, [(H + k_h)(b + k_b) - 2A_s, Cos\theta]\sqrt{H + k_h} \quad (2)$$

$$C_a=1.0333 + 0.003848\theta - 0.000045\theta^{2} \quad (3)$$

where, C_a stands for the effect of weir inclination angle, C_r represents the of upstream crest edge curvature, C_d is the discharge coefficient for vertical weir, H is the water head on the crest (m), b is the crest length (m), K_h and K_b are the correction factors for respectively water head and the effective length of the weir (m), A_s is the area of the seals (m^2), and θ is the angle of the weir with respect to the channel bed (degree). The results showed that C_a was not related to the ratio of H/P. The results also showed that the discharge coefficient increases with reducing the gate angle up to 40 degrees, but then decreases. By comparing the calculated and experimental results, the error was measured to be 6.4%. Manz [9] developed the irrigation conveyance system simulation (ICSS) model for automation of the pivot weirs and proposed a formula for C_a under free-flow conditions.

$$C_a = -10^{-12} \times 5.89\theta^6 + 10^{-9} \times 1.202\theta^5 - 10^{-8} \times 8.35\theta^4 + 10^{-6} \times 3.422\theta^3 - 10^{-4} * 2.217\theta^2 + 10^{-3} \times 9.035\theta + 1 \quad (4)$$

Prakash & Shivapour [10] performed experimental studies on flow over inclined "V" notch triangular sharp-crested weirs with the angles of 0, 15, 30, 45 and 60 degrees. Based on the experimental results, distinct equations were provided for each weir angle to estimate the discharge coefficient. Hargreaves et al. [11] evaluated the implementation of VOF (control volume) method for free flow conditions on broad-crested weirs. Standard K-ϵ and RNG K-ϵ models were studied for turbulence simulation in Fluent software. Aydin et al. [12] presented the discharge-head equations in terms of contraction ratio and weir height for vertical rectangular weirs with partially contracted and slit weirs. Zhang et al. [13] proposed a new method for calculating the sharp-crested rectangular weir discharge at the low head flow regime and drew the head-discharge curves. They mentioned that flow regime can be classified into three districts, including free flow, bistable and clinging flow regions. The classical head-discharge relation for rectangular sharp-crested weirs is applicable only to free flow conditions, and is valid at low head flow when it becomes clinging. In the bistable zone, the head–discharge relationship can be covered partly by the classical weir–discharge equations of free flow. In the clinging flow regime (with a head of less than 1 cm), discharge was directly proportional to weir width, independent of weir height. Gharahjeh et al. [14] performed experimental studies on vertical sharp-crested rectangular weirs with different side contractions and presented the equations for weir discharge coefficients. The experimental setup consists of a 6 m long flume with a width of 32 cm and depth of 70 cm. The range of the available water head (h) for this study was between 1 cm to 54 cm. Due to aeration problem, it was not possible to record discharges corresponding to heads smaller than 1 cm. Water head was measured at a distance of 2.2 m (3-4 times the water head) upstream of the weir section to get rid of the water drawdown effect, based on Bos recommendations [3]. Sheikh Rezazadeh Nikou et al. [15] presented the simple discharge-head equations for pivot weirs for free and submerged conditions. By comparing the results of extracted equation with the experimental data, the accuracy of the proposed equation for free flow conditions was obtained in the range of ±15%. BijanKhan & Ferro [16] used Buckingham's dimensional theory to simplify the equations of broad-crested rectangular weirs (with sloping walls at upstream and downstream), pivot weirs, and triangular weirs and to achieve high-precision equations. Ahmed and Aziz [17] simulated the flow through side spillways with Ansys CFX software. They pointed out that the K-ϵ and RNG K-ϵ models present appropriate results for different flow discharges, compared to the laboratory information. Bijankhan & Ferro [18] performed experimental and numerical simulations to investigate the effect of rectangular weir inclination angle for free flow condition. The experimental observations revealed that C_a increases with the inclination angle to a maximum of 1.082 for 30° of inclination. A 2D numerical

analysis by Open FOAM computational fluid dynamic toolbox and k-ϵ turbulence model was also used. They proposed the following equation for a given upstream depth:

$$C_a = (1+ \frac{0{,}041*\theta^{-21{,}348}}{206{,}9+0{,}759963\theta^{-21{,}348}})^{3/2} \quad (5)$$

According to the results, C_a obtained by experiment is slightly less than those reported by Wahlin [7] and Manz [9]. They mentioned that, for very low head (the upstream flow depth of about 2.5 cm) the effect of viscosity and poor nappe aeration can significantly affect the flow condition. Also, the maximum flow magnification ratios of 8.2% and 9.3% were observed for respectively the experimental and numerical results. Farzin et al. [19] simulated the flow over a rectangular sharp-crested weir with three angles of 50, 70, and 90 degrees, using $Flow_{3D}$ software and presented equations for the weir discharge coefficient. They showed that K-ϵ model with a correlation coefficient of 0.96 is the best turbulence model for such simulation. Azimfar et al. [20] conducted a research on the discharge coefficient of pivot weirs in free and submerged flows with analytical methods. The equations presented for both free and submerged flow are based on Bernoulli and momentum equations. The comparison of the results showed that the presented equations have less complexity and higher accuracy. The above research showed that momentum equation is applicable for free and submerged flow and Bernoulli equation is applicable only for free flow. They used the experimental results of Wahlin & Replogle [8] and Sisman [4] to calibrate and estimate the coefficients in the above relationships. Mahdavi et al. [21] performed SPH analysis on free flow in pivot weirs. Their research showed that the position of the vena contracta is transferred downstream in the steeper slopes of the weir. In addition, they proposed the following relationship for the discharge coefficient. They announced that increasing the weir angle will decrease the discharge coefficient.

$$C = 6.33*10^{-7}\theta^{3} - 6.929*10^{-5}\theta^{2} - 0.001768\,\theta + 0.9308 \quad (6)$$

Kaixuan et al. [22] studied three types of lifting systems and optimized the hydraulic mechanism for new steel gates. FRESNO (in USA) and Rubicon (in Australia) Companies also produced a pivot weir that can be connected to automatic control systems. Beijing IWHR Corporation (BIC) also introduced hydraulic elevator dams. Sinclair [23] conducted a numerical analysis on hinged overflows with $Flow_{3d}$ software in the form of his master's thesis. They studied the velocity and pressure profiles and discharge coefficients. Three types of operating regimes were identified. In high acceleration-regime for H/P less than 0.6, flow accelerates near the weir and leads to negative pressure. The ideal-regime occurs at H/P between 0.6 and 2.0 and does not experience acceleration and surging flow. Discharge coefficient is also fixed in this regime. The inundated -regime also occurs at H/P greater than 2.0, and in this case the weir is always submerged. He announced that in the ideal performance regime, each angle has its own discharge coefficient and its minimum value is at 72 degrees and maximum at 27 degrees. In a laboratory study, Ali Foroudi and Reza Barati [24] studied the changes of the cavitation index by considering the change of the convergence angle of the side walls of the ogee spillway. In this research, as the flow rate increased, the cavitation index relatively declined at both crest and chute of the spillway while growing at its toe. They declared the lowest value of cavitation index as 1.54.

In this study, Ansys CFX software was used for flow simulation. This software is used for numerical solution of two- and three-dimensional fluid flows, movable structures, multiphase flows and fluid structure interaction (FSI) using several turbulence models.The selection of the software has been done according to its capabilities compared to similar software and the integration of its various features (in the form of Ansys software package).

The main purpose of this article is to model the flow passing through single pivot weirs and to investigate the effect of weir angle on hydraulic parameters. The results are a basis for research on two and three consecutive pivot weirs. In this research, two independent variables (weir angle and another hydraulic characteristic) have been used to derive discharge equations and discharge coefficient. According to the mentioned goals, after evaluating the efficiency of Ansys CFX software, in order to integrate the research, different turbulence models and the shape of the crest were conducted simultaneously in the form of a research. In the studies conducted, the K-ε standard turbulence model was finally considered as the selected model [25]. However, in previous studies on sharp-crested weirs, the above cases were done separately and with different software.

2. Dimensional analysis

The discharge coefficient of pivot weirs is a function of geometric, kinematic and dynamic variables including: weir height (P), channel width (B), crest length (b), upstream hydraulic head (H), discharge (Q), velocity (V), gravity acceleration (g), dynamic fluid viscosity (μ), surface tension (σ) and specific gravity (ρ). Dimensional analysis is used to determine the relationship between the discharge coefficient and other effective parameters. Using Buckingham's π theory and based on non-dimensional analysis for free flow condition, the following equation for C can be presented:

$$C = f(H/P, b/B, \theta, R_e.W_e) \tag{7}$$

where, R_e is the Reynolds number and W_e is the Weber number. By measuring the hydraulic parameters, relationship between discharge coefficient and the dimensionless parameters is extracted, which can be used for different weir conditions.

2.1. Main approaches for CFD modelling

One of the main approaches to solve turbulent equations is the Reynolds Averaging of Navier-Stokes (RANS) methods. There are several models of RANS in Ansys CFX software. In this study, according to the previous and similar investigations, Standard K-$e$turbulence model was selected. The K-ε model uses two equations to solve the kinetic energy of the turbulence (K) and the eddy dissipation rate (ε) in the following forms (Liu et al. [26]) :

$$\frac{\partial}{\partial t}(\rho k) + \frac{\partial}{\partial x_i}(\rho k u_i) = \frac{\partial}{\partial x_i}\left[(\mu + \frac{\mu_t}{\sigma_k})\frac{\partial k}{\partial x_j}\right] + G_k + G_b - \rho\epsilon - Y_M + S_k \tag{8}$$

$$\frac{\partial}{\partial t}(\rho\varepsilon) + \frac{\partial}{\partial x_i}(\rho\varepsilon u_i) = \frac{\partial}{\partial x_j}\left[(\mu + \frac{\mu_t}{\sigma_\epsilon})\frac{\partial \epsilon}{\partial x_j}\right] + C_{1\epsilon}\frac{\epsilon}{k}(G_k + G_b, C_{3\epsilon} - C_{2\varepsilon}\rho\frac{\varepsilon^2}{k} + S_\epsilon \tag{9}$$

where, G_k and G_b are respectively the energy production due to mean velocity gradients and buoyancy, Y_M is the kinetic energy production due to flow compression (zero for incompressible flows), σ_k and σ_ε are Prandtl numbers for k and ε, and S_k and S_ε are source terms (can be defined by the operator). In the above equations, the values of $C_{1\epsilon}$, $C_{2\epsilon}$, $C_{3\epsilon}$, s_k *and* s_e are constant coefficients equal to 1.44, 1.92, 0.09, 1.0 and 1.3, respectively. μ_t is also the eddy viscosity which is equal to $\rho c_\mu \frac{k^2}{\epsilon}$.

The control volume method is usually used to analyze multiphase flows (including two or more immiscible fluids). In this method, interface between the two phases is determined and the volume fraction of each fluid in each cell is calculated in the domain. The volume ratio of each phase in the control volume is equal to the percentage of volume occupied by each phase. Therefore, in each control volume, the sum of volume fractions in all phases is equal to 1. The volume fraction of fluid in a cell (q) is expressed as α_q with the following conditions:

- $\alpha_q = 0$: The cell is empty.
- $\alpha_q = 1$: The cell is full of fluid q.
- $0 < \alpha_q < 1$: The cell contains a common surface between fluid q and one or more other fluids.

3. Material and Methods

Experimental data of USBR (United States Bureau of Reclamation) on Armtec gates were used to evaluate the model results [8, 25]. According to the experimental results, the model was applied for different Armtec pivot weir angles and flow discharges. The length and height of the flume were considered 200 and 65 cm, respectively. With side contraction equal to 0.925, the width of the flume and the length of the weir were 123 and 114 cm, respectively. Standard K-ε method was also used as the turbulence model. The output results are presented in Table 1.

Table 1. Output results on experimental data of Armtec pivot weir

Geometry and hydraulics parameters	Unit	Run No.				
		1	2	3	4	5
Q	lit/s	62.22	65.35	27.92	149.57	61.47
θ	degree	63.4	43.6	43.6	22.4	22.4
Y	cm	52.5	44.3	39.7	37.8	29.6
Y_{USBR}		52.3	43.7	39.6	36.3	29.4
RE	%	0.3	1.3	0.2	4.4	0.6
RMSE	-	0.17	0.56	0.09	1.58	0.18

In the table, the *USBR* index represents the values of the hydraulic parameter based on the laboratory data. The relative error and the root mean square error between the model and laboratory was respectively calculated between 0.2 to 4.4% and 0.17 to 1.58, which showed reasonable performance of the model.

3.1. Domain and geometry

Flow geometry including flume and weir was plotted using Ansys Workbench. Weir dimensions and hydraulic parameters were considered in accordance to Table 2. In order to facilitate the modeling, a length scale (L_r) of $\frac{1}{5}$ was used for simulation. All geometric and hydraulic parameters were scaled based on L_r ($=L_m/L_p$) and Q_r ($=Q_m/Q_p = L_r^3$), where p and m represent the prototype and model specifications, respectively. The results are shown in Table 3. It is observed that the weir has no side contraction. Due to the symmetry of the flow domain (Figure 2), the model was run for half of the flume (see Figure 3). The shape of the crest was also drawn as a semicircle (see Figure 2).

Table 2. Prototype geometric characteristics and hydraulic parameters

Discharge (m^3/s)	Angle (º)	Weir dimensions (m)			Flume dimensions (m)		
Q	Θ	t	b	H_w	h	B	L
16.25,10 and 5	90,70,50 and 27.8	0.1	6	2	2.5 and 3.25	6	10

Table 3. Model geometric characteristics and hydraulic parameters

Discharge (m^3/s)	Angle (º)	Weir dimensions (m)			Flume dimensions (m)		
Q	Θ	t	b	H_w	h	B	L
130,80 and 40	90,70,50 and 27.8	2	120	40	50 and 65	120	200

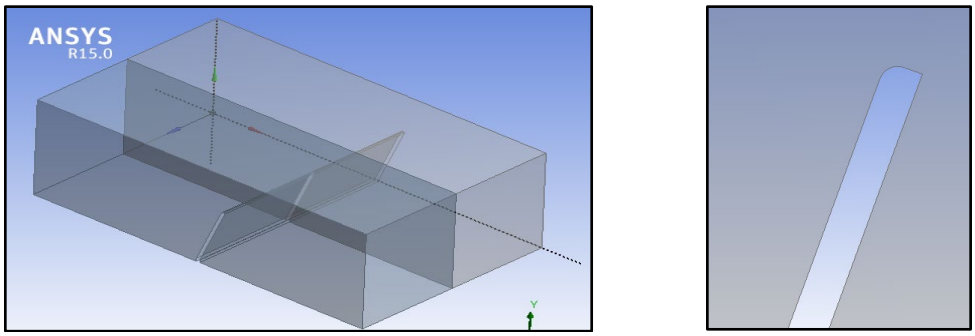

Figure 2. Flume and pivot weir and symmetry plane and shape of crest

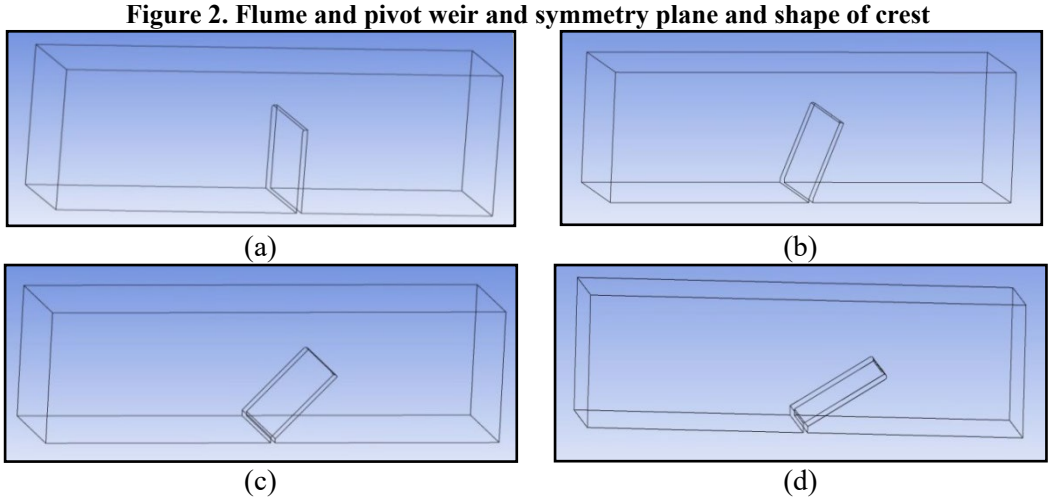

Figure 3. Semi-flume and weir with angles of (a) 90º; (b) 70º; (c) 50º and (d) 27.8º

All boundaries were divided and introduced in the model. Accordingly, Inlet area shows the inflow area upstream of the flume (Figure 4a), where the flow discharges is determined as the inlet condition. Outlet area shows the outflow area downstream of the flume (Figure 4b), where the static pressure is defined equal to zero. The upper surface of the control volume (Figure 4c) is defined as the open surface in order to establish the possibility of air-water flux. Also, relative pressure is considered equal to zero. The Symmetry conditions apply to the parts of the domain where there are geometric and physical symmetries. The boundary surface between two halves of the domain is defined as the symmetry surface (Figure 4d). Except all defined boundary surfaces, the rest of the boundaries are considered as wall, which represents solid surfaces. Due to the type of flow conditions in this research, no-slip condition is used at walls.

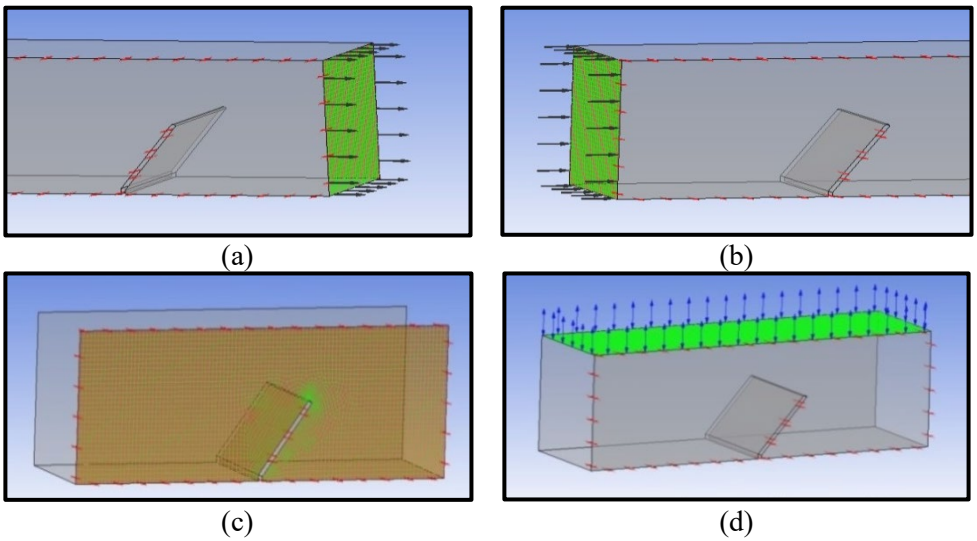

Figure 4. Position of borders: (a) input, (b) output, (c) symmetry, (d) opening,

3.2. Model preparation

The mesh sensitivity control was initially performed for a flow discharge of 80 lit/s and an angle of 27.8 degrees to select the optimal mesh size. For this purpose, the size of the domain mesh was changed by 20% (from 2 cm to 1.6 cm). The results showed less than 0.6% variation in calculated upstream water surface of the weir was, which is insignificant. Therefore, a 2 cm mesh was used for flow domain, while a fine mesh size was considered at the edge and near to the weir.

Due to the change in hydraulic parameters during the model implementation, the flow was selected as "Transient". As mentioned before, the standard K-ϵ turbulence model was used. In this study, the "Total Time" option was used to determine the execution time. The model execution time was estimated 17 and 18 s, which shows almost zero upstream water surface fluctuation. In this research, the high resolution option has been used to discretize the equations.

Air and water were selected as the two flow phases (fluid types). In part of the flume upstream of the weir, where it is always full of water, the water volume fraction is considered as 1. This assumption reduced the solution time.

Sisman [4], Zhang et al. [13], Gharajeh et al. [14] and Bijankhan et al. [18] suggested the minimum water depth on the weir (H) to avoid the effect of viscosity, clinging flow and poor aeration as 2.0, 1.0, 1.0 And 2.5 cm, respectively. In this study, the minimum value of H was obtained equal to 6.4 cm, which is more than the minimum values recommended in previous studies.

4. Results and discussion

After preparing the model, it was run for specified weir angles and flow discharges. The model outputs are presented in Table 4. According to the previous investigations (Bos [3]; Gharajeh et al. [14]), the best point for reading the water level is 3 to 4 times H above the weir. So, the water surface level was read at a suitable distance upstream of the weir. Figure 5 shows a sample of water surface profile over the weir. In Table 4, the discharge coefficient is calculated based on the width, the height, and the angle of the weir and the upstream water depth. In this table, the effect of weir inclination angle C_a is assumed equal to 1 for $\theta=90$ degrees, and then the values of C_a were calculated for different angles.

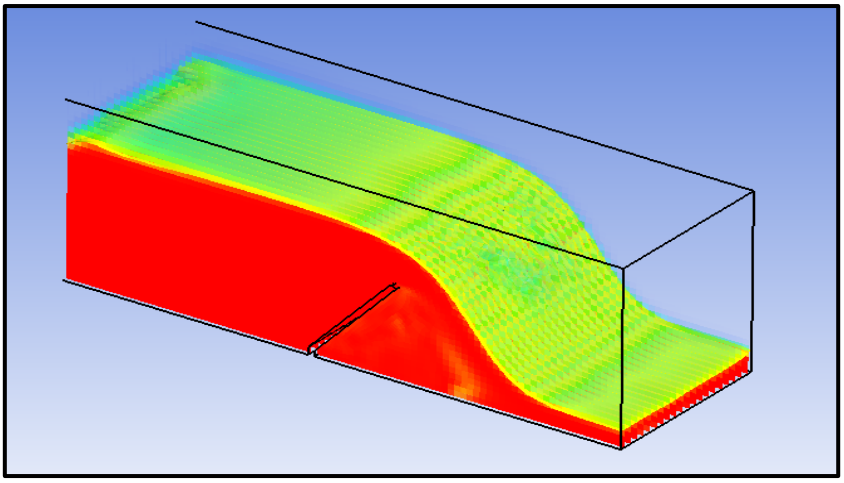

Figure 5. Sample water surface profiles for spillway

Table 4. Calculation of discharge coefficient of pivot weirs

Geometry and hydraulics parameters	Unit	Number of runs											
		1	2	3	4	5	6	7	8	9	10	11	12
Q	lit/s	130	130	130	130	80	80	80	80	40	40	40	40
θ	°	90	70	50	27.8	90	70	50	27.8	90	70	50	27.8
P	cm	41.6	39.9	33.8	22.7	41.6	39.9	33.8	22.7	41.6	39.9	33.8	22.7
Y	cm	59.4	57.0	50.8	39.9	53.7	51.5	45.6	34.7	48.1	46.3	40.2	29.2
H	cm	17.8	17.1	17.0	17.2	12.0	11.6	11.8	12.0	6.5	6.4	6.4	6.5
H/P	cm	0.43	0.43	0.50	0.76	0.29	0.29	0.35	0.53	0.16	0.16	0.19	0.28
C	-	0.487	0.519	0.524	0.515	0.540	0.568	0.557	0.543	0.680	0.698	0.696	0.689
R_e	-	54041	55172	58262	64620	34950	35610	37618	18685	18685	18685	18685	18685
C_a	-	1.000	1.067	1.076	1.058	1.000	1.053	1.033	1.007	1.000	1.026	1.024	1.012

Figures 6 to 8 show the variation of flow discharge and discharge coefficient against the water depth (Y in the upstream), water head (H on the weir crest) and ratio of water head on the crest to weir height (H/P).

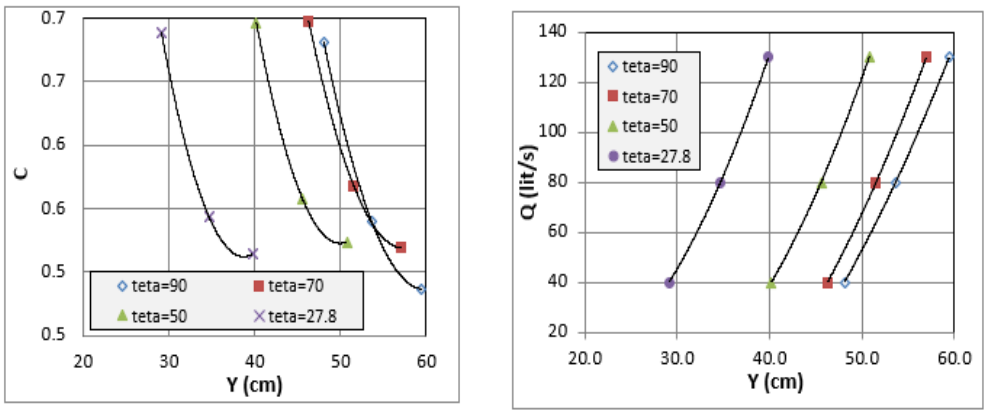

Figure 6. Variation of *C* and *Q* versus Y (cm)

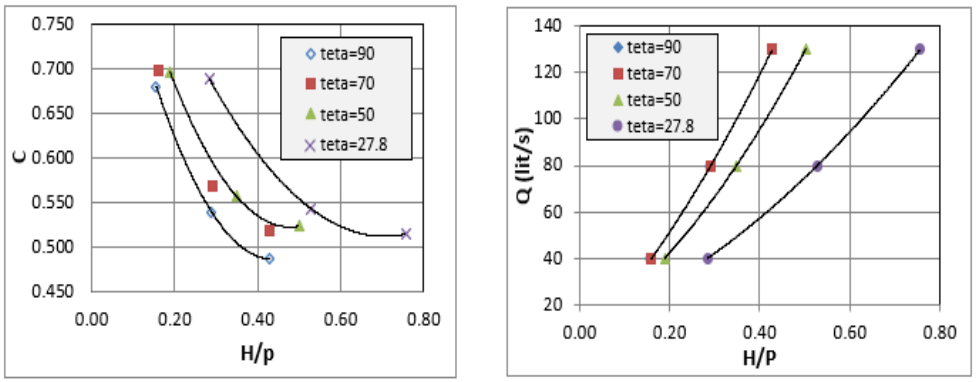

Figure 7. Variation of *C* and *Q* versus H/P

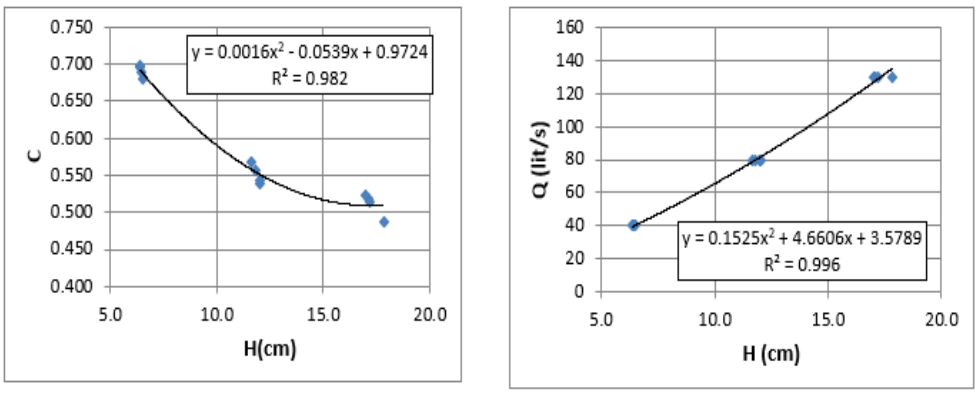

Figure 8. Variation of *C* and *Q* versus H (cm)

In this research, the results were presented in two parts. The first part was for the validation of model and software implementation. In this regard, Ca coefficients for different angles were calculated and the results were presented in the last row of Table 4 and Figures 9 and 10. In the second part, based on the results presented in Table 4 and the graphs drawn, the necessary analyzes were performed and the final results were presented in Tables 5 and 6. Then, the benefits of using these weirs, especially during floods, were investigated.

PART 1:

As explained before, the effect of weir inclination angle C_a =1 was assumed for θ=90° and then, C_a was calculated for different angles (Table 4). The trend in C_a variation for different flow discharges is also shown in Figure 9.

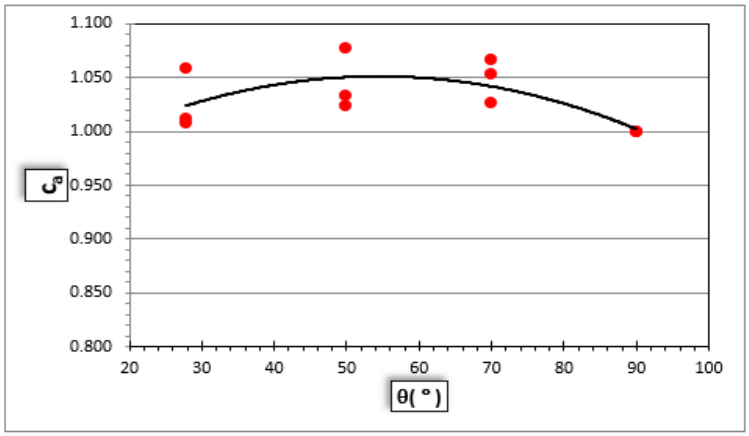

Figure 9. Variation of C_a coefficients in terms of θ for different discharges

By fitting the C_a - Θ curve, the following equation is derived:

$$C_a=0.9364 + 0.0042\theta - 0.000040\theta^2 \quad (10)$$

As can be seen in Figure 9 and Equation 10, C_a for a specific flow discharge increases as the weir angle reduces to 52°, but then decreases by further declining the weir angle. This is consistent with the results of previous studies (Wahlin [7]; Bijankhan [17]). The maximum value of C_a was found equal to 1.076, which showed a slight difference with the results of Wahlin [7], Manz [8] and Bijankhan [17]. They presented the maximum values of C_a as 1.121, 1.110 and 1.082, respectively. This difference can be caused by the difference in the shape and hydraulic conditions of the weirs. The comparison of C_a based on Wahlin and Manz (Equation 3 and 4) and the present studies is shown in Figure 10.

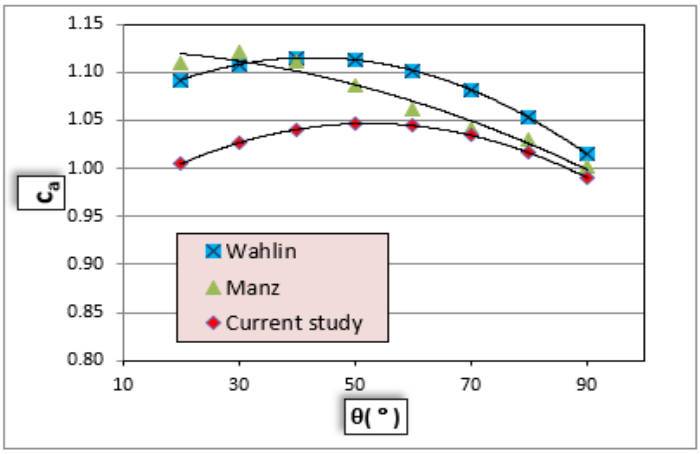

Figure 10. Comparison of C_a variation for different studies

PART 2:

The variations of (*C-Y*), (*C-H/P*), (*Q-Y*) and (*Q-H/P*) curves for different weir angles were observed in Figures 6 to 8. The figures show a relatively definite correlation between *C* and *Q* and *Y* and *H/P* . Therefore, it was tried to provide specific relationship for each series of the curves. In this regard, *C* or *Q* parameters are considered as dependent variables and *Y*, H/P and θ are considered as independent variables. According to Table 4 information and using LAB Fit Curve Fitting software, different equations were derived. Based on the relative and root mean square values of errors, the most appropriate equations for each curve were derived. Chi-square test was used to evaluate the curve fitting. If the calculated coefficient is much larger than 1, it indicates a poor fitting and if the chi-square value is around 1, it indicates the good consistency between observations and predictions. The values smaller than 1 indicate a very good consistency.

The (*C-H*) and (*Q-H*) curves in Figure 8 show the possibility of developing two equations with and without applying the weir angle. Table 5 presents the resulted equations as a function of weir angle, using LAB Fit Curve Fitting software. Table 6 also shows the relevant equations independent of weir angle, using Excel software. By analyzing the correlation coefficient and the relative and root mean square values of errors, the most appropriate equations are presented with a good consistency with the model results.

Table 5. Developed eequations for discharge and discharge coefficient

Eq. NO.	Dependent variable	Independent variables	Equation	Relative Error Percent	Root Mean Square Error	Fit Chi Squared Coefficient
11	C	$\theta.Y$	$C=1260.1EXP(\frac{-117,43}{\theta}-0,153Y)+0.465$	0.3 to 3.6	0.0 to 0.04	0.0005
12			$C=\frac{1}{-1,345+0,05*Y+\frac{38,1}{\theta}}$	0.2 to 5.9	0.0 to 0.04	0.0006
13	Q	$\theta.Y$	$Q=0.039\,\theta^2-7,15\theta+8,12Y-28,91$	0.3 to 14.8	0.3 to 6.5	12.9
14			$Q=-7.07\theta+0,039\theta^2+6,78Y+0,014Y^2$	0.2 to 7.9	0.1 to 5.7	17.6
15	C	$\theta.H$	$C=1.555*\theta^{\left(-0,262+\frac{0,648}{H}\right)}-\frac{6,309}{\theta}$	0.1 to 1.9	0.0 to 0.01	0.0001
16			$C=\frac{1}{2,232+0,00039\theta-\frac{5,2}{H}}$	0.1 to 4.0	0.0 to 0.02	0.0001
17	Q	$\theta.H$	$Q=0,286\theta-0,0027\theta^2+4,18H+0,17H^2$	0.0 to 3.0	0.0 to 2.6	1.7
18	C	$\theta.H/P$	$C=0.253*(\frac{H}{P})^{(-0,407-7,95/\theta)}+0.279*\frac{H}{P}$	0.2 to 3.6	0.0 to 0.02	0.0001
19			$C=3.017*\theta^{\left(-1,45(\frac{H}{P})^{0,487}\right)}+0.462$	0.6 to 3.2	0.0 to 0.02	0.0001
20	Q	$\theta.H/P$	$Q=\frac{-5,19+105,56\frac{H}{P}}{1-0,018\theta+0,00012\theta^2}$	1.1 to 19.6	0.9 to 16.1	17.0

Table 6. Equations of discharge and weir discharge coefficient using Excel software

NO.	Dependent variable	Independent variables	Equation	Relative Error Percent	Root Mean Square Error	Correlation coefficient R^2
21	C	$\theta.H$	C =0.0016*H^2-0.0539*H+0.9724	0.1 to 6.9	0.0 to 0.03	0.982
22	Q	$\theta.H$	Q =0.1525*H^2+4.6606*H+3.5789	0.0 to 4.1	0.0 to 5.3	0.997

The results of Table 4 and the discharge-head equations presented in Tables 5 and 6 show that if the upstream water depth is assumed equal to 59.4 cm, the weir discharge capacity increases by reducing the weir angle from 90° to 27.8°. The result has been summarized in Table 7 (assuming a constant upstream water depth). Variation of calculated discharge versus weir angle is shown in Figure 11. An exponential increase in the weir capacity with a further decrease in weir angle is evident in the figure.

Table 7. Overflow discharge for upstream constant water depth

Angle (º)	P (cm)	Y (cm)	H (cm)	Q (lit/s)		Percentage increase in discharge (%)	
				Eq. 17	Eq. 22	Eq. 17	Eq. 22
90	41.6	59.4	17.8	132	135	-	-
70	39.90	59.4	19.5	153	152	15.7	13.0
50	33.80	59.4	25.6	226	223	71.0	65.2
27.8	22.70	59.4	36.7	388	380	193.8	181.8

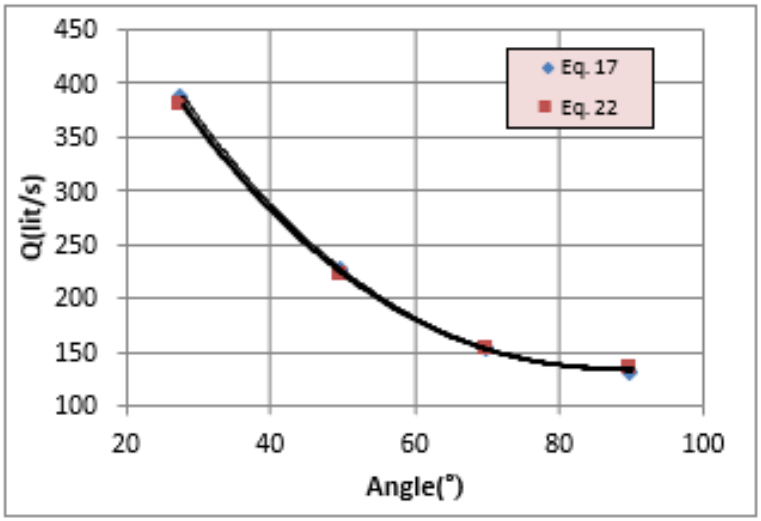

Figure 11. Variation of discharge versus weir angle for upstream constant water depth (H=59.4 cm)

5. Conclusion

In this study, observing the trend of changes in the values of the Ca coefficient with respect to different angles and discharges showed that the highest value equal to 1.076 is obtained for an angle of 52 degrees. This coefficient first increases and then decreases with the decrease of the weir angle. This problem showed a good agreement with previous studies for pivot weirs (with different shapes and hydraulic conditions).

In other words, at lower slopes, the discharge coefficient increases due to the smoother flow lines passing over the spillway. In weirs, due to the formation of the stagnation zone, the energy of the flow lines is reduced when they collide with the weir surface, and a secondary flow is created near the weir, and the discharge coefficient can be affected by this flow. The effect of these secondary flows is high at higher angles, in other words, the flow coefficient of the pivot weir is high at low angles and decreases with the increase of the angle.

After running the model for different discharges and angles, discharge curves and discharge coefficient were drawn with respect to Y, H, H/P, and θ variables and equations with high correlation coefficient were extracted. The presented Q-Y equations showed that (in a constant Y value in the weir upstream channel) if the weir is inclined by 60 degrees from the vertical state, the flow passing over the weir increases exponentially. For example, for Y = 0.54, the flow rate of the weir will be about 2.8 to 2.9 times after the 60 degree change. In other words, by keeping the water depth in the upstream channel constant during the flood, damage to the upstream lands is prevented.

As mentioned, in the selection of the discharge values and dimensions of the weir, an effort was made to observe the minimum water depth on the weir based on the standards and recommendations of previous researchers. So, the minimum water depth on these weirs was considered equal to 6 cm. Therefore, it is necessary to carry out studies on the weir for lower discharges and lower water depth. Examining the amount of negative pressure behind the overflow body indicated that the cavitation index was within the permissible limit. However, it is suggested to conduct research to reduce the cavitation index and negative pressure of other forms of overflow crown and other solutions.

References

1. King, H. W., Wisler, C. O., and Woodburn, J. G. (1948) Hydraulics, Wiley, New York.
2. Rehbock, T. (1929) Discussion of Precise Weir measurements. By Turner, K.B, Transactions of the American Society of Civil Engineers, 93(1), 1143-1162, https://doi.org/10.1061/TACEAT.0004045
3. Bos MG. (1989) *Discharge Measurement Structures*. Third revised edition. International Institute for Land Reclamation and Improvement, Wageningen, the Netherlands.
4. Sisman, HC. (2009) *Experimental Investigation on Sharp-Crested Rectangular Weirs*. M.Sc.Thesis, Department of Civil Engineering, Middle East Technical University, Ankara (Turkey).
5. Hulsing, H. (1968) *Measurement of peak discharge at dams by indirect method*. USBR, Chapter A5, Book 3, Applications of hydraulics.
6. Swamee, P. K. (1988) Generalized Rectangular Weir Equations. *Journal of Hydraulic Engineering*, *114*(8), 945–949. https://doi.org/10.1061/(asce)0733-9429(1988)114:8(945)
7. Kindsvater, C.E., and Carter, R W. (1959). "Discharge Characteristics of Rectangular Thin-Plate Weirs." *ASCE.,* Vol. 124, Issue 1, p. 772-822.0

8. Wahlin, B. T. and Replogle, J. A. (1994) *Flow Measurement Using an Overshot Gate*. *U.S. Dept. of the Interior Bureau of Reclamation, Denver*, (1425). https://doi.org/10.1080/09715010.2003.10514735
9. Manz, D. H. (1985). "Systems analysis of irrigation conveyance systems." M.SC. thesis, Univ. of Alberta, Edmonton, AL, Canada.
10. Shesha Prakash, M. N. and Shivapur, A. V. (2003) Flow over inclined sharp crested triangular weir. *ISH Journal of Hydraulic Engineering*, 9(2), 80–88.
11. Hargreaves, D. M., Morvan, H. P. and Wright, N. G. (2007) Validation of the Volume of Fluid Method for Free Surface Calculation: The Broad-Crested Weir. *Engineering Applications of Computational Fluid Mechanics*, *1*(2), 136–146. https://doi.org/10.1080/19942060.2007.11015188
12. Aydin, I., Altan-Sakarya, A. B. and Sisman, C. (2011) Discharge formula for rectangular sharp-crested weirs. *Flow Measurement and Instrumentation*, *22*(2),144–151. https://doi.org/10.1016/j.flowmeasinst.2011.01.003
13. Zhang, X., Yuan, L., Yan, P., Li, J. and He, X. (2015) Rectangular sharp-crested weir calibration for low head and clinging flow regime. *Irrigation Science*, *33*(2), 131–139. https://doi.org/10.1007/s00271-014-0453-1
14. Gharahjeh S. Aydin I. Altan Sakarya A. B. (2012) Discharge Formula for Sharp-Crested Rectangular Weirs. *10th International Congress on Advances in Civil Engineering, Middle East Technical University, Ankara, Turkey*(*2012*).
15. Sheikh Rezazadeh Nikou, N., Monem, M. J. and Safavi, K. (2016) Extraction of the Flow Rate Equation under Free and Submerged Flow Conditions in Pivot Weirs with Different Side Contractions. *Journal of Irrigation and Drainage Engineering*, *142*(8), 04016025. https://doi.org/10.1061/(asce)ir.1943-4774.0001027
16. Bijankhan, M. and Ferro, V. (2017) Dimensional analysis and stage-discharge relationship for weirs. A review. *Journal of Agricultural Engineering*. 48(1), 1-11. https://doi.org/10.4081/jae.2017.575
17. Ahmed S. and Aziz W. (2018) Numerical Modeling of Flow in Side Channel Spillway Using ANSYS-CFX. *ZANCO Journal of Pure and Applied Sciences*. 30(s1), DOI: 10.21271/zjpas.30.s1.10
18. Bijankhan, M., & Ferro, V. (2018). Experimental Study and Numerical Simulation of Inclined Rectangular Weirs. *Journal of Irrigation and Drainage Engineering*, *144*(7), 04018012. https://doi.org/10.1061/(asce)ir.1943-4774.0001325
19. Farzin S. Karami H. Yahyavi F. (2018) Numerical Study of Hydraulic Characteristics Around the Vertical and Diagonal Sharp-Crested Weirs Using FLOW3D Simulation. *Journal of Civil Infrastructure Researches,* 4(1), 15-24. doi: https://dx.doi.org/10.22091/cer.2017.1661.1068
20. Azimfar, S. M., Hosseini, S. A., & Khosrojerrdi, A. (2018). Derivation of discharge coefficient of a pivot weir under free and submergence flow conditions. Flow Measurement and Instrumentation, 59, 45–51. https://doi.org/10.1016/j.flowmeasinst.2017.11.010

21. Mahdavi, A., & Shahkarami, N. (2020). SPH Analysis of Free Surface Flow over Pivot Weirs. *KSCE Journal of Civil Engineering*, *24*(4), 1183–1194. https://doi.org/10.1007/s12205-020-0095-1
22. Kaixuan, L., Yehan, G., Zhan, W., & Yongsheng, Y. (2021). Research and Calculation on the Optimization of Hydraulic Lifting Mechanism for New Steel Gate. *IOP Conference Series: Earth and Environmental Science*, *643*, 012136. https://doi.org/10.1088/1755-1315/643/1/012136
23. Sinclair, J. M. (2021). New insights into flow over sharp-crested and pivot weirs using computational fluid dynamics.
24. Foroudi, A., & Barati, R. (2022). Experimental study of cavitation index in an ogee spillway by considering convergence angle of sidewalls. *Water Supply*. https://doi.org/10.2166/ws.2022.228
25. Khatamipour, B., & Khosrojerdi, A., & Kavianpour, M., & Ghodsihassanabad, M. (2022). Simulation of two-phase turbulent flow of pivot weirs with different crest shapes. Water and Soil Resources Conservation. 10.30495/wsrcj.2022.19227
26. Liu, C., Huhe, A. and Ma, W. 2002. Numerical and experimental investigation of flow over a semicircular weir. Acta Mechanica Sinica/Lixue Xuebao, 18(6): 594–602. https://doi.org/10.1007/bf02487961